HBT correlation in 158 A·GeV Pb+Pb collisions

R. Ganz for the NA49 collaboration

Max-Planck-Institut für Physik München, Föhringer Ring 6, D-80805 München, Germany

E-mail: ganz@mppmu.mpg.de

H. Appelshäuser[7,#], J. Bächler[5], S.J. Bailey[17], D. Barna[4], L.S. Barnby[3], J. Bartke[6], R.A. Barton[3], H. Białkowska[15], A. Billmeier[10], C.O. Blyth[3], R. Bock[7], C. Bormann[10], F.P. Brady[8], R. Brockmann[7,†], R. Brun[5], P. Bunčić[5,10], H.L. Caines[3], D. Cebra[8], G.E. Cooper[2], J.G. Cramer[17], M. Cristinziani[13], P. Csato[4], J. Dunn[8], V. Eckardt[14], F. Eckhardt[13], M.I. Ferguson[5], H.G. Fischer[5], D. Flierl[10], Z. Fodor[4], P. Foka[10], P. Freund[14], V. Friese[13], M. Fuchs[10], F. Gabler[10], J. Gal[4], R. Ganz[14], M. Gaździcki[10], E. Gładysz[6], J. Grebieszkow[16], J. Günther[10], J.W. Harris[18], S. Hegyi[4], T. Henkel[13], L.A. Hill[3], I. Huang[2,8], H. Hümmler[10,+], G. Igo[12], D. Irmscher[2,7], P. Jacobs[2], P.G. Jones[3], K. Kadija[19,14], V.I. Kolesnikov[9], M. Kowalski[6], B. Lasiuk[12,18], P. Lévai[4] A.I. Malakhov[9], S. Margetis[11], C. Markert[7], G.L. Melkumov[9], A. Mock[14], J. Molnár[4], J.M. Nelson[3], M. Oldenburg[10], G. Odyniec[2], G. Palla[4], A.D. Panagiotou[1], A. Petridis[1], A. Piper[13], R.J. Porter[2], A.M. Poskanzer[2], S. Poziombka[10], D.J. Prindle[17], F. Pühlhofer[13], W. Rauch[14], J.G. Reid[17], R. Renfordt[10], W. Retyk[16], H.G. Ritter[2], D. Röhrich[10], C. Roland[7], G. Roland[10], H. Rudolph[2,10], A. Rybicki[6], A. Sandoval[7], H. Sann[7], A.Yu. Semenov[9], E. Schäfer[14], D. Schmischke[10], N. Schmitz[14], S. Schönfelder[14], P. Seyboth[14], J. Seyerlein[14], F. Sikler[4], E. Skrzypczak[16], G.T.A. Squier[3], R. Stock[10], H. Ströbele[10], Chr. Struck[13], I. Szentpetery[4], J. Sziklai[4], M. Toy[2,12], T.A. Trainor[17], S. Trentalange[12], T. Ullrich[18], M. Vassiliou[1], G. Veres[4], G. Vesztergombi[4], D. Vranić[5,19], F. Wang[2], D.D. Weerasundara[17], S. Wenig[5], C. Whitten[12], T. Wienold[2,#], L. Wood[8], T.A. Yates[3], J. Zimanyi[4], X.-Z. Zhu[17], R. Zybert[3]

[1] *Department of Physics, University of Athens, Athens, Greece.*
[2] *Lawrence Berkeley National Laboratory, University of California, Berkeley, USA.*
[3] *Birmingham University, Birmingham, England.*
[4] *KFKI Research Institute for Particle and Nuclear Physics, Budapest, Hungary.*
[5] *CERN, Geneva, Switzerland.*
[6] *Institute of Nuclear Physics, Cracow, Poland.*
[7] *Gesellschaft für Schwerionenforschung (GSI), Darmstadt, Germany.*
[8] *University of California at Davis, Davis, USA.*
[9] *Joint Institute for Nuclear Research, Dubna, Russia.*
[10] *Fachbereich Physik der Universität, Frankfurt, Germany.*
[11] *Kent State University, Kent, OH, USA.*
[12] *University of California at Los Angeles, Los Angeles, USA.*
[13] *Fachbereich Physik der Universität, Marburg, Germany.*
[14] *Max-Planck-Institut für Physik, Munich, Germany.*

[15] *Institute for Nuclear Studies, Warsaw, Poland.*
[16] *Institute for Experimental Physics, University of Warsaw, Warsaw, Poland.*
[17] *Nuclear Physics Laboratory, University of Washington, Seattle, WA, USA.*
[18] *Yale University, New Haven, CT, USA.*
[19] *Rudjer Boskovic Institute, Zagreb, Croatia.*
† *deceased.*
# *present address: Physikalisches Institut, Universitaet Heidelberg, Germany.*
+ *present address: Max-Planck-Institut für Physik, Munich, Germany.*

The large acceptance TPCs of the NA49 spectrometer allow for a systematic multidimensional study of two-particle correlations in different part of phase space. Results from Bertsch-Pratt and Yano-Koonin-Podgoretskii parametrizations are presented differentially in transverse pair momentum and pair rapidity. These studies give an insight into the dynamical space-time evolution of relativistic Pb+Pb collisions, which is dominated by longitudinal expansion.

1 Introduction

Recent high statistics experiments have demonstrated that, in heavy ion collisions at relativistic beam energies, a single characteristic radius from intensity interferometry does not exist. First of all one deals with systems, in which the emission of particles is distributed over various ranges in three dimensional space as well as in time. Secondly, due to the dynamical behaviour of the source (eg. collective expansion) correlations arise between the momenta of particles and the point of emission in space-time, which results in a dependence of HBT radii on kinematical quantities. In the case of a "boost invariant" picture, first suggested by Bjorken[1], the hot and dense initial stage of the collision expands longitudinally until freeze-out such, that a distinct longitudinal velocity (v_z) profile is established: $v_z = z/t_f$. Here, z is the distance of particle emission at freeze-out from the center of the collision and t_f the freeze-out time. With respect to HBT correlations – appearing at low momentum differences of particle pairs – such a velocity profile disconnects different parts of the source along the beam axis. Only additional thermal motion with average velocities of $< v_{therm} > \approx \sqrt{T/m_\perp}$ can – over certain distances – compensate for the longitudinal velocity gradient. This means that, in case of relativistic heavy ion collisions, HBT radii do not measure the geometry of the source, but a "length of homogeneity" [2] $dz = R_z = t_f \sqrt{T/m_\perp}$, which may vary inside the source and hence depend on the phase space in which the pairs are observed.

Experimentally, the question of space-time size of the source is addressed by extracting HBT radii for all space-time components of the momentum difference vector $q^\mu = p_1^\mu - p_2^\mu; \mu = 0..3$ of pairs of identical particles 1 and 2. Unfortunately, the "on-mass-shell"- constraint for the observed (real) parti-

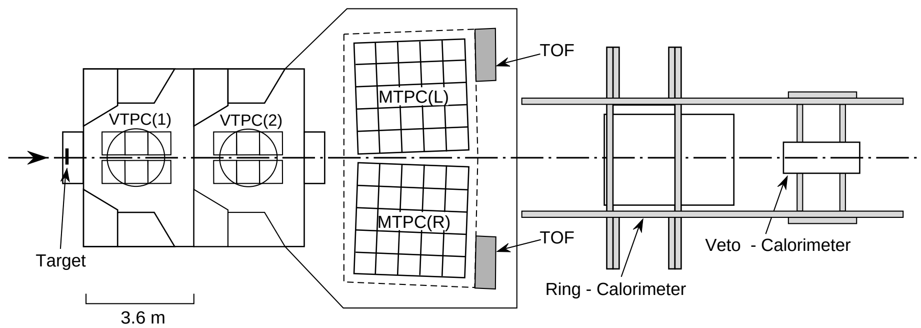

Figure 1: The NA49 spectrometer

cles reduces the degrees of freedom to three. For pairs this constraint can be written as

$$q_0 k_0 = \vec{q}\vec{k} \tag{1}$$

with the average pair momentum $k^\mu = (p_1^\mu + p_2^\mu)/2$. Later it will be shown how this condition is utilized to eliminate one of the four space-time components of q^μ to deduce parametrizations of the three dimensional correlation function $C_2(q)$ according to Bertsch-Pratt(BP [3]) or to Yano-Koonin-Podgoretskii (YKP [4]).

The second point – the dynamical space momentum correlation – is investigated experimentally by carrying out full three dimensional HBT analyses for intervals in the average transverse pair momentum ($k_\perp$) and average pair rapidity ($y = (y_1 + y_2)/2$), separately. All together this can be expressed by (q components introduced in section 3):

$$C_2(q^\mu) \longrightarrow C_2(q^\mu, k^\mu) = C_2\left(\begin{bmatrix} BP : q_{side}, q_{out}, q_{long} \\ YKP : q_\perp, q_0, q_{||} \end{bmatrix}, [k_\perp, y]\right) \tag{2}$$

Such a detailed analysis requires of course a large data sample over a large fraction of phase space. Facilitated by the large number of particles produced in central Pb+Pb collisions at 158 A·GeV and the large acceptance of the NA49 spectrometer at the CERN SPS accelerator such a study has become feasible and is presented here.

2 NA49 spectrometer and data analysis

The NA49 spectrometer[5] (figure 1) is located in the North area of the CERN SPS. The results presented here are derived from the run period in 1995 with a 158 A·GeV Pb-beam. In every spill (5 s) about 10^5 Pb^{82+} ions impinge on a

224 mg/cm^2 Pb-target. 1% of these projectiles interact with the nuclei of the target foil. The most central 5% (impact parameter $b = 0 - 3.5$ fm) of these collision are selected by the NA49 trigger utilizing a *Veto- Calorimeter*, which measures the energy carried by the beam spectator fragments. In such central collision about 1200 charged particles are produced, roughly 800 of them are detected in at least one of the four *TPC*s (Time Projection Chambers) of NA49. At 2.0 m and 5.8 m downstream of the target two smaller chambers (*VTPC1, VTPC2*; volume=$2.0 \times 0.7 \times 2.5$ m^3) are placed inside magnetic dipole fields. In the "Standard Configuration" the fields amount for 1.5 Telsa (*VTPC1*) and 1.1 Tesla (*VTPC2*), respectively, whereas in case of the "Low field configuration", fields of 0.3 Tesla and 1.5 Tesla have been used, shifting the acceptance for pions towards central rapidities. Further downstream – outside the magnetic field – the acceptance is extended to forward rapidities and higher momenta by two large volume TPCs' (*MTPC*; volume=$3.8 \times 1.2 \times 3.8$ m^3).

All four *TPC*s are equipped with a charge sensitive read-out, highly segmented along the beam (z-axis) and perpendicular to it in horizontal direction (x-axis). For each of these 180.000 pads the charge is determined in 512 consecutive time slices (100 ns), to determine the vertical (y-axis) position of particle tracks via the drift velocity ($v_d \approx$1.4 cm/μs inside *VTPC* and $v_d \approx$2.2 cm/μs inside *MTPC*). This scheme allows for 3-dimensional track reconstruction. From the curvature of reconstructed tracks inside the *VTPC* the momentum of particles is determined to a precision of $\delta p/p^2 \approx 0.3\%$ in addition to their charge. Moreover, all chambers measure the energy (dE/dx) deposited by the particle in the detector gas, which – in a future stage of analysis – will be used to identify the particles. For the HBT analysis presented here, pairs of hadrons of the same charge (h^-h^- or h^+h^+) without further identification have been considered. These are dominated by pairs of identical pions ($\pi^-\pi^-$ or $\pi^+\pi^+$). It has been shown, that a contamination from other particles has negligible influence on the determination of HBT radii, with the exception of the chaotic parameter λ, which will not be discussed in this article.

Independent analyses have been carried out for the *VTPC2* and the *MTPC*s. The *VTPC2* analysis[6] is based on 40.000 central Pb+Pb collisions, half of them taken in the "Low field configuration" and the other half in "Standard field configuration". The analysis of the *MTPC* data[7] includes the same 40.000 events and adds another 50.000 events in "Standard field configuration". In both analyses pairs of tracks with distances less than 2 cm inside the TPC have been excluded to eliminate the influence of two particle reconstruction inefficiency for very close tracks. The same requirement has been imposed on the distribution of uncorrelated pairs, which is generated by combining tracks from different events. This distribution is used as reference (denominator) in the determination of the correlation function. Both data sets have been corrected for Coulomb final state interaction based on measured correlations of opposite-sign charged particles. In case of the *VTPC2*–data this correction is carried out by the Gamov factor $G(q_{inv}); q_{inv} = \sqrt{-(p_1 - p2)^2}$ modified by a dumping term to account for the finite size of the source [8]:

$$C_{2,corr}^{--} = C_{2,meas.}^{--} \times \Big((G(q_{inv}) - 1)e^{-q_{inv}/q_{eff}} + 1\Big) \tag{3}$$

The parameter q_{eff} is determined from a fit of the 1-dimensional correlation function $C_2^{+-}(q_{inv})$.

The *MTPC*–data are corrected by the correlation function C_2^{+-} of the opposite charged particles, evaluated in the same three dimensionial relative momentum space as the like-sign pairs; eg. for BP-paramertization (see below):

$$C_{2,corr}^{--} = C_{2,meas.}^{--} \times C^{+-}(q_{side}, q_{out}, q_{long}) \tag{4}$$

No further corrections have been applied to the data. The systematic error in the determination of the HBT radii is estimated to about 7%. The correlations function have been obtained in different reference frames. The most intuitive choice of a reference frame for all pair momenta might be the **C**enter- of **M**ass **S**ystem (CMS) of the colliding ions, but in case of variations of the longitudinal velocity across the source due to a longitudinal expansion, the **L**ongitudinal **C**o-**M**oving **S**ystem (LCMS) might be better suited. It is defined on a pair-by-pair basis such that the longitudinal pair momentum $k_\parallel$ vanishes. The **F**ixed **L**ongitudinal **C**o-**M**oving **S**ystem (FLCMS), in which the observer frame for every interval in pair rapidity is fixed at the center of that interval, might be seen as a compromise between both. In case of narrow widths of rapidity intervals LCMS and FLCMS are equivalent and are therefore treated as one in the following discussion, even though the *MTPC* data [7] have been evaluated in the CMS and FLCMS frames, whereas the *VTPC2* data [6] use the CMS and LCMS frames for BP projections and CMS and FLCMS in case of YKP.

3 Q- parametrizations

As shown in references [9,10], the correlation function for a source distribution, expanded to second order at the (in general k-dependent) space time points of maximum emission ($\bar{X}$; saddle point) can be written as:

$$C_2 = 1 + e^{-q^\mu q^\nu <\hat{x}_\mu \hat{x}_\nu>} \tag{5}$$

with $\hat{x}_\mu = x_\mu - \bar{X}_\mu$; $<>$ denotes an averaging over the source distribution. Even though this "model independent" expression (5) can – because of the

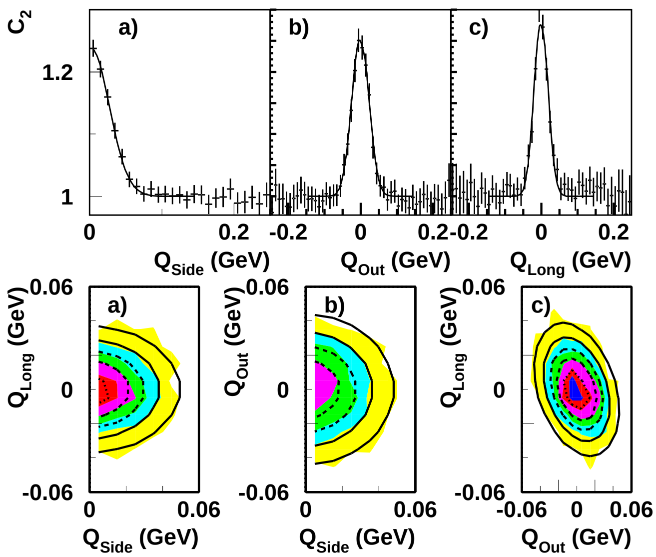

Figure 2: 1- and 2-dimensional projections of the $h^- h^-$ correlation function measured in the NA49 *MTPC* using BP parameters for pair rapidities $4 < y < 5$ and transverse momenta $k_\perp < 100$ MeV/c (FLCMS). The projections on components q_j have been carried out by restricting the other components $q_i; i \neq j$ to $q_i < 30$ MeV/c.

constraint in eq. (1) – not be used to describe measured correlation functions, it is a generalization of both the Bertsch Pratt [3] as well as the Yano Koonin Podgoretskii parametrization. It therefore gains its importance as a tool when interpreting the radii extracted in the framework of both formulations; it furthermore provides a proof of consistency, when comparing results from both parametriztions.

3.1 BP parametrization

Eliminating the temporal component of (5) by condition (1) in the form $q_0 = \vec{\beta}\vec{q}$ ($\vec{\beta} = \vec{k}/k_0$), results in a correlation function parametrized according to reference [3]:

$$C_2 = 1 + \lambda e^{-q_{side}^2 R_{side}^2 - q_{out}^2 R_{out}^2 - q_{long}^2 R_{long}^2 - 2q_{out}q_{long}R_{out-long}^2} \tag{6}$$

Here q_{long} is the component of q^μ in beam direction, whereas q_{side} and q_{out} are those perpendicular to it, with $q_{out} \| \vec{k}$ and $q_{side} \perp \vec{k}$.

Due to symmetries of the sources considered here, only the "out–long" cross term remains, all others ("out–side" and "side–long") vanish. This is consistent with the experimental observation presented in figure 3 for h^-h^--pairs at rapidities $4 < y < 5$ and transverse pair momentum $k_\perp < 100$ MeV/c. The contours lines in the 2-dimensional projection deviate from a circular shape (no cross term correlation) only in case of the "out–long" projection. The 1-dimensional projections demonstrate the good agreement between the function (6) and the data for small q, where the correlation signal is clearly visible, as well as for larger q, where the data points are consitent with $C_2 = 1$ within the error-bars. At this point it should be emphasized, that all HBT radii presented here are derived by a simultaneous fit of all three components of q in C_2. The projections are generated for better visibility only.

When interpreting the BP radii it is advantageous to explicitly write down the relation between equation 6 and ansatz 5:

$$R^2_{side}(\vec{k}) = < \hat{x}_y^2 > \tag{7}$$

$$R^2_{out}(\vec{k}) = < (\hat{x}_x - \beta_\perp \hat{t})^2 > \tag{8}$$

$$R^2_{long}(\vec{k}) = < (\hat{x}_z - \beta_\parallel \hat{t})^2 > \tag{9}$$

$$R^2_{out,long}(\vec{k}) = < (\hat{x}_x - \beta_\perp \hat{t})(\hat{x}_z - \beta_\parallel \hat{t}) > \tag{10}$$

With the exception of R_{side}, BP-radii mix spacial ($\hat{x}_{xyz}$)and temporal components ($\hat{t}$) of the source and an interpretation becomes therefore reference frame and model dependent. In case of a longitudinally expanding source the "length of homogeneity" observed in the center of mass frame, appears Lorentz contracted in different intervals of pair rapidity. Such a behaviour is supported by the rapidity dependence of the measured radius R_{long}, as shown for different intervals in $k_\perp$ in figure 3. The data points can be described by $R_{long} = t_f/\mathrm{cosh(y)}\sqrt{\mathrm{T/m_\perp}}$, which is the Lorentz frame dependent expression of section 1. Assuming a temperature of $T = 150$ MeV, a freeze-out time of $t_f \approx 9 - 7$ fm/c can be derived for the different $k_\perp$-intervals. By comparing the measured "*side*"- and "*out*"-radii to equation (8)-(7) the duration time of freeze-out yields $\approx 2-4$ fm/c. Both radii ("*side*" and "*out*") appear to be constant over $y < 2.5$ within errors. In addition to the physical interpretation it is important to note the good overall agreement between the different analyses and between pairs of opposite total charge, i.e. h^-h^- compared to h^+h^+.

3.2 YKP parametrization

Instead of eliminating the temporal component of (5) in the BP formalism, condition (1) might also be used via the relation $q_x = q_0/\beta_\perp - q_\parallel \beta_\parallel/\beta_\perp$. With the picture of a boost invariant source in mind with different parts of the source moving at different longitudinal velocities, one explicitly introduces a

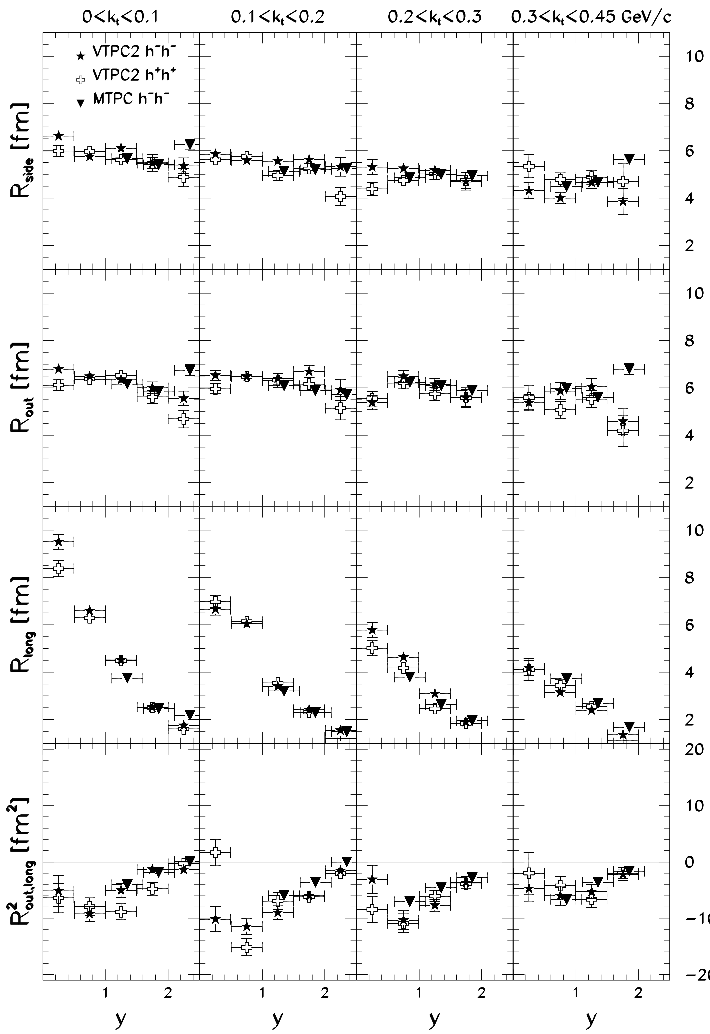

Figure 3: The dependence of BP radii on the pair rapidity for h^-h^--pairs ($\star$) and h^+h^+-pairs ($+$) in the *VTPC2* and h^-h^--pairs ($\bigtriangledown$) in the *MTPC* in four intervals of transverse momentum k_t (CMS). The rapidity scale is shifted to the center of mass system of the ions. The horizontal error bars correspond to the width of the intervals chosen in the analysis and the vertical to the statistical errors only.

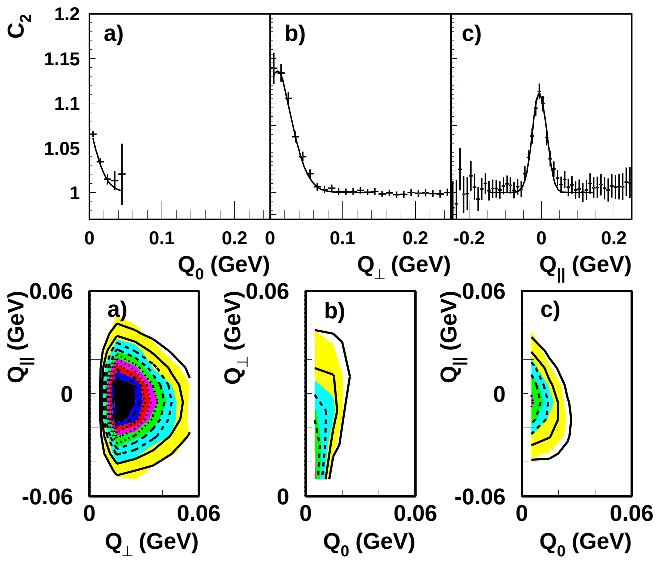

Figure 4: Projections of the same data sample as in figure 2, but this time in the YKP parametrization (FLCMS). The projection onto component(s) q_j have been carried out by restricting the other component(s) $q_i; i \neq j$ to $q_i < 70$ MeV/c.

longitudinal velocity parameter (β_{YKP}) into the correlation function of YKP type [4]:

$$C_2 = 1 + \lambda e^{-q_\perp^2 R_\perp^2 - \gamma_{YKP}^2 (q_\parallel - \beta_{YKP} q_0)^2 R_\parallel^2 - \gamma_{YKP}^2 (q_0 - \beta_{YKP} q_\parallel)^2 R_0^2} \tag{11}$$

with $\gamma_{YKP} = 1/\sqrt{1-\beta_{YKP}^2}$, $\quad q_\perp = \sqrt{q_x^2 + q_y^2}$ for the transverse momentum difference, q_0 for the energy difference and $q_\parallel$ for the longitudinal component. In this case the interpretation of extracted radii becomes more evident, since space and time components are decoupled (the validity of the approximation is discussed in reference [11]):

$$R_\perp^2(\vec{k}) = <\hat{x}_y^2> \tag{12}$$

$$R_0^2(\vec{k}) \approx <\hat{t}^2> \tag{13}$$

$$R_\parallel^2(\vec{k}) \approx <\hat{x}_z^2> \tag{14}$$

Figure 4 shows one and 2-dimensional projections of the measured correlation function in YKP coordinates evaluated in the LCMS frame for the same $k_\perp$ and y-interval as in figure 2. Again, the data are described well by the chosen gaussian ansatz. A problem of this type of parametrization manifests itself

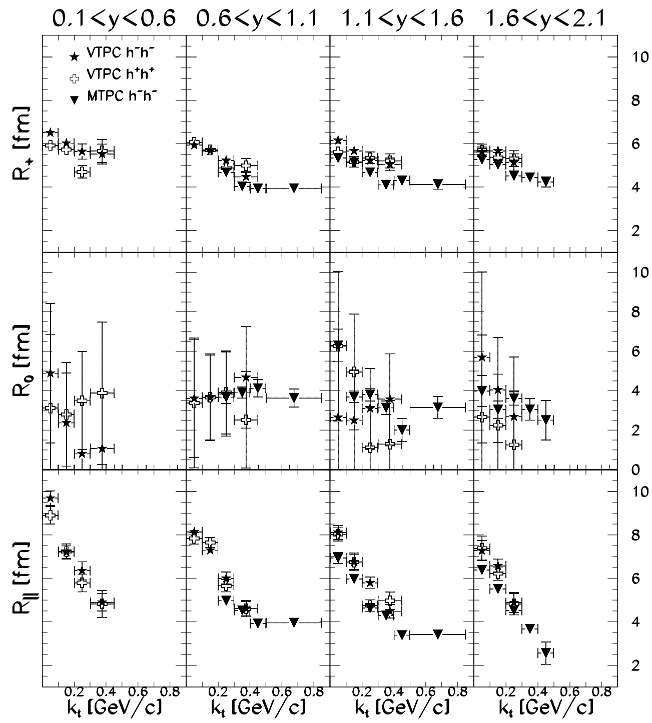

Figure 5: The dependence of YKP-HBT radii on the transverse pair momentum $k_\perp$ in different intervals of pair rapidity (LCMS) (otherwise same conventions as in figure 5).

in the projection of q_0. For a given interval in $q_\perp$ and $q_\parallel$ only a limited region of q_0 is kinematically available. This is the reason for the large uncertainties of R_0 in figure 5, which sumarizes the k_t-dependence for the YKP-radii in different intervals of rapidity. The clear decrease of $R_\parallel$ vs. k_t again points to strong space-momentum correlations in the source. Moreover, even in the transverse direction $R_\perp$ decreases for larger k_t-values, which can be interpreted by transverse flow [12]. The estimate of the duration of emission given in section 3.1 is confirmed by the extracted values of R_0.

In a parametrization of YKP type one can gain further insight into the dynamics of the source by utilizing the YKP velocity β_{YKP}. The YKP rapidity $y_{YKP} = \frac{1}{2}\ln\frac{1+\beta_{YKP}}{1-\beta_{YKP}} + y$ derived from the measured β_{YKP} is compared to the pair rapidity in figure 6. The data show the characteristics of a source, which expands in longitudinal direction. Even though deviations from an ideal boost invariant picture (line in figure 6), become apparant at forward rapidities, the

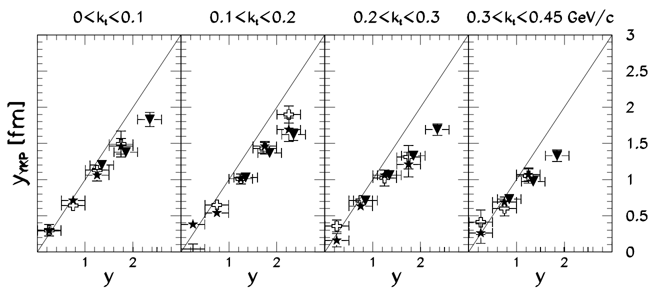

Figure 6: Dependence of the Yano Koonin rapidity vs. the pair rapidity for four intervals in $k_\perp$ (LCMS).

consitstency which such a model is good.

4 Conclusion and Outlook

Results from different analyses of multidimensional Bertsch-Pratt and Yano-Koonin-Podgoreskii parametrizations of two particle correlation functions in 158 A·GeV Pb+Pb collisions have been presented differentially in pair rapidity y and transverse pair momentum k_t. The results confirm the importantance of extracting HBT-radii seperately in different parts of phase space to disentangle the dynamical correlations of the source. The pion source appears to expand in a close to boost invariant way, as seen in the rapidity dependence of the Yano-Koonin velocity as well as of the R_{long} radius in the CMS system. Moreover, a finite duration time of emission of $2-4$ fm/c and a decreasing tranverse radius at large k_t are observed. For a better understanding of the behaviour of the radii a comparison to a similar analysis of proton-proton and proton-lead collisions is currently in progress. Moreover, the centrality dependence and beam energy dependence might constrain interpretations even further and will be investigated in upcoming analysis and further data taking.

Acknowledgments

Acknowledgements: This work was supported by the Director, Office of Energy Research, Division of Nuclear Physics of the Office of High Energy and Nuclear Physics of the US Department of Energy under Contract DE-ACO3-76SFOOO98, the US National Science Foundation, the Bundesministerium fur Bildung und Forschung, Germany, the Alexander von Humboldt Foundation, the UK Engineering and Physical Sciences Research Council, the Polish State Committee for Scientific Research (2 P03B 01912), the Hungarian Scientific Research Foundation under contracts T14920 and T23790, the EC Marie Curie

Foundation, and the Polish-German Foundation.

References

1. J.D. Bjorken, *Phys. Rev.* D **27**, 140 (1983).
2. Yu. M. Sinyukov *et el.*, *Nucl. Phys.* A **498**, 151 (1989) and *Nucl. Phys.* A **566**, 589 (1994).
3. G. F. Bertsch, *Nucl. Phys.* A **498**, 173 (1989); S. Pratt, *Phys. Rev.* D **33**, 1314 (1986).
4. F. B. Yano and S.E. Koonin, *Phys. Lett.* B **78**, 556 (1978); M.I. Podgoretskii, *Sov. J. Nucl. Phys.* **37**, 272 (1983) S. Chapman, P. Scotto and U. Heinz, *Phys. Rev. Lett.* **74**, 4400 (1995).
5. P. Seyboth *et al.*, *Proc. of XXV Int. Symposium on Multiparticle Dynamics* Stara Lesna Slovakia, 170 (1995).
6. H. Appelshäuser, PhD thesis, Univ. Frankfurt a.M. (1997).
7. S. Schönfelder, PhD thesis, MPI München MPI-PhE/97-09 (1997).
8. K. Kadija *et el.*, *Nucl. Phys.* A **610**, 248 (1996).
9. S. Chapman *et al.*, *Phys. Rev.* C **52**, 2694 (1995).
10. U. Heinz *et al.*, *Phys. Lett.* B **382**, 181 (1996).
11. Y.F. Wu *et al.*, *Euro. Phys. J.* C **1**, 599 (1998).
12. H. Appelshäuser *et al.*, *Euro. Phys. J.* C **2**, 611 (1998).